Photonuclear reactions in $^{40}Ca^{\dagger}$

D. Brajnik, D. Jamnik, G. Kernel, U. Miklavžič, and A. Stanovnik
J. Stefan Institute, University of Ljubljana, Ljubljana, Yugoslavia
(Received 29 January 1974)

Natural calcium targets were bombarded with γ rays from a 31-MeV betatron at several bremsstrahlung end-point energies. Angular and energy distributions of photoprotons were measured. In addition, the γ-ray spectra emerging from the thick target were recorded at several angles. They were used to study the γ rays accompanying the decay of excited residual nuclei formed in the reactions $^{40}Ca(\gamma,p)$ and $^{40}Ca(\gamma,n)$. The analysis yielded the following results for the main reaction channels: the energy dependence of the cross sections, the energy dependence of photoproton angular distributions, and the bremsstrahlung-weighted angular distributions of deexcitation γ rays. According to the experimental results the following amplitudes seem to dominate in the particle channels: $f_{5/2}$ waves for the (γ,p_0) reaction, $p_{3/2}$ waves for (γ,p_1), and p waves for reaction channels in which the residual nuclei are left in states above 4.93 MeV. This is consistent with the giant dipole state configuration, predicted on the basis of the shell-model bound-state calculation by Gillet and Sanderson. The agreement with continuum theories is less satisfactory. It is also found that the shapes of cross sections are more uniform and that the angular distributions are less energy-dependent than expected from theory. The (γ,p_1) cross section was separated into $S=0$ and $S=1$ channel spin contributions of which only the dominant $S=0$ part shows a resonant structure. Negative-parity hole channels bear evidence for two-step reaction processes and impurities in the ground state of ^{40}Ca. Ratios of (γ,p) and (γ,n) cross sections imply an admixture of less than 3% of $T=0$ strength in the ^{40}Ca giant dipole resonance.

[NUCLEAR REACTIONS $^{40}Ca(\gamma,p)$, $(\gamma,p\gamma')$, and $(\gamma,n\gamma')$, $E_\gamma=11$–30 MeV; measured $\sigma(E,\vartheta)$ to states of residual nuclei; deduced reaction-channel configurations.]

I. INTRODUCTION

Experimental work related to the photonuclear giant dipole resonance (GDR) is most frequently limited to measurements in which properties of reaction channels involving excited states of residual nuclei cannot be studied. This stems mainly from experimental difficulties connected with the separation of reaction products. On the other hand, in the extensively investigated ground-state–to–ground-state transitions, the experimental precision and details exceed the scope of present calculations based on reaction theories and nuclear models. It is believed, therefore, that the experimental work directed to the study of reaction channels involving residual nuclei in definite states would help to improve the understanding of photonuclear processes. In particular, it is expected that to a large extent the configuration of the giant dipole state is preserved in particle-hole reaction channels. Of special interest, therefore, are the closed-shell nuclei, where a good knowledge of the configurations of the states involved exists, and a simpler interpretation of the experimental data is anticipated.

In the present work a study of photonuclear reactions on the nucleus ^{40}Ca was undertaken with the aim of providing lacking information of the discussed type. A number of reaction processes accessible by the Ljubljana betatron facilities were investigated in a combined experiment in which photoproton spectra from the (γ,p) reaction and γ-ray spectra from the $(\gamma,p\gamma')$ and $(\gamma,n\gamma')$ reactions were measured. These were used to deduce the energy dependence of the cross sections, angular distributions, and the configurations of reaction channels involving residual nuclei in different states.

II. EXPERIMENTAL PROCEDURE

Since the details of the experimental setup and method were discussed elsewhere[1] only a brief description is given here. Two independent experiments were performed on two separate natural calcium targets (Fig. 1).

A thin (6.5 mg/cm^2) calcium target located in a vacuum chamber at a distance of 1.23 m from the source of betatron bremsstrahlung radiation was used for the measurement of proton spectra. Protons were detected at four different angles with respect to the direction of the incident γ-ray beam: 30, 81.4, 98.6, and 150°. In the analysis, spectra from the two closely spaced angles at 81.4 and 98.6° were combined and treated as 90°

data. Target thickness determined almost entirely the energy resolution which consequently varied with detector angle. At a proton energy of 10 MeV it was 220 keV for the 90° angle and 320 keV for 30 and 150°. Background was kept low by adequate shielding, precise collimation, and magnetic cleaning fields in the vacuum chamber (for electron and positron suppression). Pulses were collected only during the time intervals determined by the duration of bremsstrahlung bursts.

For the measurement of the deexcitation γ-ray spectra resulting from the reactions $(\gamma, n\gamma')$ and $(\gamma, p\gamma')$, a thick calcium target (8 cm × 8 cm × 6 cm) was used. The target was located in a shielded area outside the accelerator room (Fig. 1) at a distance of about 10 m from the bremsstrahlung source. Deexcitation γ rays were detected by means of a 27-cm^3 Ge(Li) counter. In order to minimize pileup caused by background, 2.2 cm of lead was placed in front of the counter. As in the case of photoprotons, the γ-ray spectrometer was gated with the betatron bremsstrahlung bursts.

Two ionization chambers with current integrators were used for monitoring the bremsstrahlung beam[1]: a transmission thin-wall ionization chamber and a thick-wall ionization chamber of the Pruitt type. The charge collected from the latter was used for determination of the photon flux[2] on which the evaluation of the absolute values of cross sections was based.

III. EXPERIMENTAL DATA AND RESULTS OF THE ANALYSIS

A. Photoproton data

Photoproton spectra measured at 10 bremsstrahlung end-point energies ranging from 15.2 to 24.6 MeV and at angles of 30, 90, and 150° are shown in Fig. 2. Cross sections for photoproton reactions to different excited states of the residual nucleus ^{39}K were extracted from the proton spectra by applying the method of least squares.[1] In the analysis, only those excited states of ^{39}K (in addition to the ground state) were included which were found to be strongly populated in the photoproton process. The extent of population was obtained from the spectra of deexcitation γ rays (see Fig. 3). The analysis of the raw experimental data included transformation to the centre-of-mass system and finite solid angle corrections. The results of the analysis are presented in the form of coefficients $4\pi A_0 = \sigma$, A_2/A_0, and $(A_1 + \frac{3}{8}A_3)/A_0$ (Figs. 4–8), obtained by fitting the angular distributions to a Legendre polynomial series

$$\frac{d\sigma}{d\Omega}(\vartheta) = \sum_{l=0}^{3} A_l P_l(\cos\vartheta).$$

The ^{39}K states of excitations above 2.82 MeV could not be resolved and, therefore, above this energy summed cross sections for groups of states are presented (Figs. 6–8). In these cases the energy resolution of the summed cross sections is impaired, since a weighted[3] mean value of excitation energies is used in the least-squares analysis. The estimated resolutions are as follows: 0.5 MeV for the group of negative-parity states $\frac{7}{2}^-$ 2.82 MeV, $\frac{3}{2}^-$ 3.02 MeV, $\frac{9}{2}^-$ 3.59, 3.88, 3.94 MeV (Fig. 6); 1 MeV for the 4.93–6.35-MeV group (Fig. 7) with main contribution from the 5.27-, 5.62-, 6.35-MeV $\frac{5}{2}^+$ states; and 1 MeV for unbound states (Fig. 8).

In the case of the (γ, p_1) reaction a separation of cross sections for channel spins 0 and 1 is possible assuming a dominant $E1$ process. The two cross sections are given by[4]

$$\sigma(S=0) = \tfrac{8}{3}\pi A_0(\tfrac{1}{2} - A_2/A_0),$$

$$\sigma(S=1) = \tfrac{8}{3}\pi A_0(1 + A_2/A_0).$$

It is seen from Fig. 9 that about 93% of the (γ, p_1) cross section is of the $S=0$ character. An attempt was also made to separate the two amplitudes in the j-j coupling scheme. Since the amplitudes $j = \frac{3}{2}$ and $j = \frac{1}{2}$ add coherently, the resulting cross section depends on the relative phase. There are, therefore, three unknown parameters (the

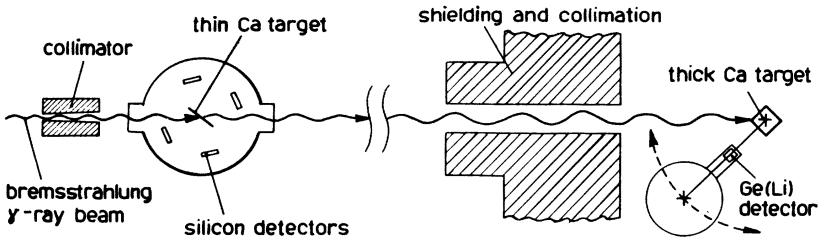

FIG. 1. Schematic drawing of the experimental arrangement.

two amplitudes and the **relative** phase between them) and only two quantities obtained from the experiment (Legendre polynomial coefficients A_0 and A_2). However, studies of inverse reactions with polarized protons[5,6] indicate a constant ratio of the two amplitudes over the giant resonance region for the studied nuclei. Assuming that such a constancy can be applied here, we find that the ratio $|p_{3/2}/p_{1/2}|^2$ between 1 and 3 would be consistent with the experimental data. Consequently, a constant ratio of 2 was used to obtain an energy dependence for the cosine of the relative phase (Fig. 10).

B. Deexcitation γ-ray data

The spectra of γ rays (an example is shown in Fig. 3) from the reactions $(\gamma, p\gamma')$ and $(\gamma, n\gamma')$ were obtained at 12 bremsstrahlung end-point energies between 14 and 31 MeV. At the highest bremsstrahlung end-point energy, angular distributions at six angles between 90 and 163° were measured, but at lower energies the angle with the bremsstrahlung beam was 135°.

The γ-ray yields of the strongly populated levels in ^{39}K (2.53, 2.82, 3.02, 3.94 MeV) and ^{39}Ca (2.47 MeV) were analyzed by the matrix inversion method of Penfold and Leiss,[7] resulting in the energy dependence of the cross sections (Fig. 11). For the evaluation of these cross sections the bremsstrahlung-weighted angular distributions measured at the 30.25-MeV bremsstrahlung end-point energy were used. In the case of other levels only energy-integrated cross sections (Table I) were calculated, assuming that the cross sections for different reaction channels were the same shape. For comparison, integrated cross sections obtained in the photoproton experiment are also listed in Table I.

The angular distribution of γ rays following a γ-particle reaction depends on the configuration of the particular reaction channel. There is strong experimental evidence that over 90% of the cross section in the region of the giant resonance is due to the electromagnetic transitions of the electric dipole type. When other transitions can be neglected, and if the spin, parity, and decay mode of the state of the residual nucleus are known, a phase space can be defined to which the possible channel configurations are restricted.

In Table II the measured ratios of Legendre polynomial coefficients A_2/A_0 are shown for several levels with γ-ray transitions to the ground state of the residual nuclei. (Only ground-state transitions gave sufficient yields for the study of angular distribution). Also spins, parities, and mixing ratios for the decay to the ground states are given in cases where such data are available.

As an example, the expression for the angular distribution of γ rays in the $\frac{7}{2}^- \rightarrow \frac{3}{2}^+$ transition has the following form[12] in the j-j coupling (only $E1$ transitions are considered in the excitation

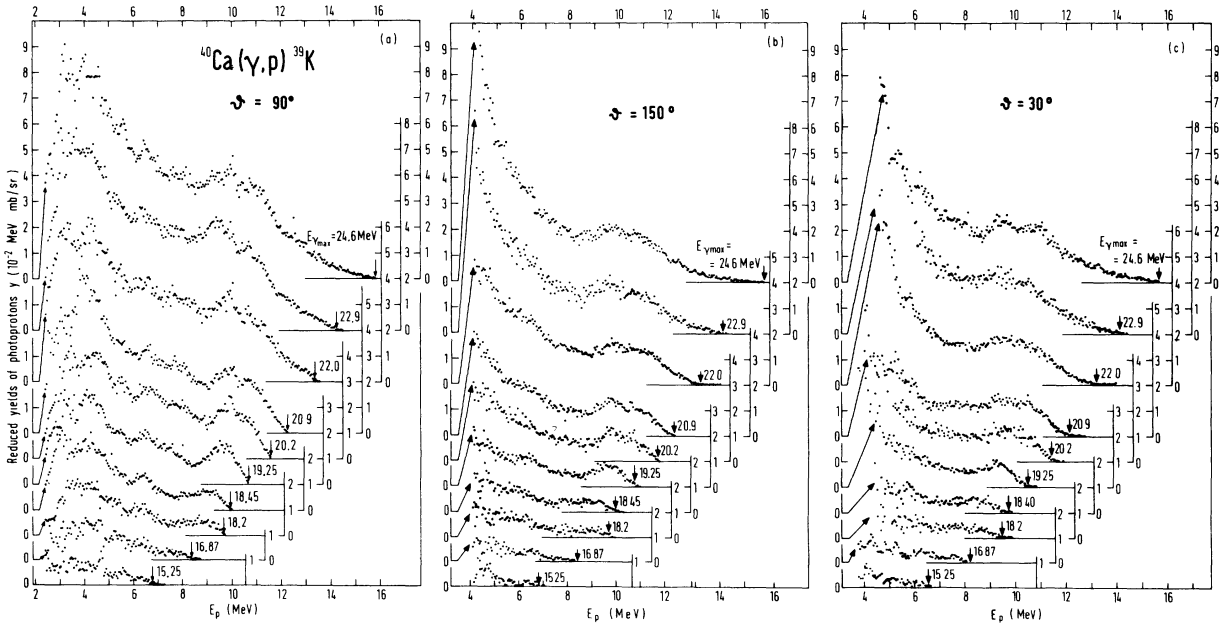

FIG. 2. (a) Photoproton spectra measured at different bremsstrahlung end-point energies $E_{\gamma max}$ at an angle 90° from the bremsstrahlung beam. (b) Photoproton spectra measured at an angle 150° from the bremsstrahlung beam. (c) Photoproton spectra measured at an angle 30° from the bremsstrahlung beam.

of ^{40}Ca):

$$\frac{W(\vartheta)}{A_0} = 1 + \frac{\frac{1}{10}\sqrt{7}\,|g_{9/2}|^2 - 2/\sqrt{21}\,|g_{7/2}|^2 + \frac{1}{2}\sqrt{\frac{3}{7}}\,|d_{5/2}|^2}{|g_{9/2}|^2 + |g_{7/2}|^2 + |d_{5/2}|^2} \frac{-\frac{5}{7}\sqrt{3} - \frac{5}{2}\delta^2/\sqrt{21} + \frac{10}{7}\delta/\sqrt{2}}{1+\delta^2} P_2(\cos\vartheta),$$

where $|g_{9/2}|$, $|g_{7/2}|$, and $|d_{5/2}|$ are amplitudes of $g_{9/2}$, $g_{7/2}$, and $d_{5/2}$ proton waves, respectively, and δ is the mixing ratio. The sign of δ is chosen according to the convention of Rose and Brink.[13] It should be noted that since the nucleons are not detected no interference terms are present in the above expression.

Angular distributions are shown in Figs. 12 and 13 for several levels. The following two mixing ratios were used for the determination of phase-space diagrams in Fig. 12: $\delta(E3/M2) = -0.19 \pm 0.10$ for the $\frac{7}{2}^- \rightarrow \frac{3}{2}^+$ transition, and $\delta(M2/E1) = 0.03$ for the $\frac{3}{2}^- \rightarrow \frac{3}{2}^+$ transition. As it can be concluded from upper diagrams in Fig. 12, the configurations of these two negative-parity-hole reaction channels are well defined by the measured angular distributions. Since the $E2/M1$ mixing ratio for the decay of the 6.35-MeV ($\frac{5}{2}^+$) state is unknown, all possible values were taken into account. Disregarding the region of the phase-space diagram where the spin-flip transition dominates, the possible configurations are determined by the upper shaded area (lower diagram of Fig. 12). A similar quantitative conclusion can be drawn for the other two $\frac{5}{2}^+$(5.27- and 5.62-MeV) states having the same A_2/A_0 values. It is seen (Table II and Fig. 12) that for the two $J = \frac{1}{2}$ first excited states of ^{39}K and ^{39}Ca the experimental data show the expected isotropic angular distributions.

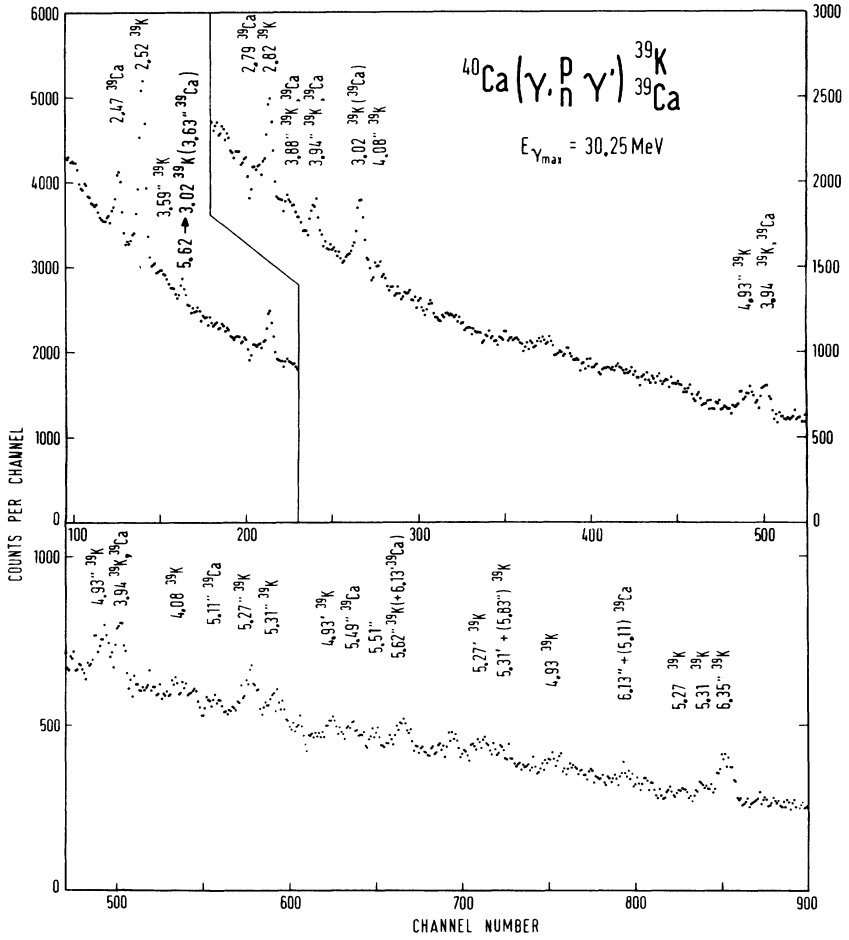

FIG. 3. Example of the deexcitation γ-ray spectra obtained at 30.25-MeV bremsstrahlung end-point energy at an angle 135° from the beam direction. Peaks are labeled by the energies of corresponding levels in the residual nuclei.

C. Evaluation of errors

In a simplified case where only one level (e.g., ground state) is populated in the photoproton reaction, the differential cross section $(d\sigma/d\Omega)(E_\gamma)$ is evaluated from the proton spectrum by use of a simple relation

$$Y(E_p, E_{\gamma_0}) = P(E_\gamma, E_{\gamma_0}) \frac{d\sigma}{d\Omega}(E_\gamma).$$

Here the reduced yield Y is the number of photoprotons per unit interval of their energy E_p normalized to the unit response of the bremsstrahlung monitor, divided by the detector effective solid angle and the number of irradiated target nuclei. $P(E_\gamma, E_{\gamma_0})$ represents the spectrum of the bremsstrahlung with maximum energy E_{γ_0} normalized to the unit monitor response.

In the general case more than one level is populated in the reaction and the right-hand side of the equation is represented by a sum over cross sections to different states in the residual nucleus. To determine these cross sections, reduced yields at several bremsstrahlung end-point energies E_{γ_0} have to be measured and a set of simultaneous equations solved. Since the general procedure of least-squares fit is described in Ref. 1, our discussion here is limited to the accuracy of the results.

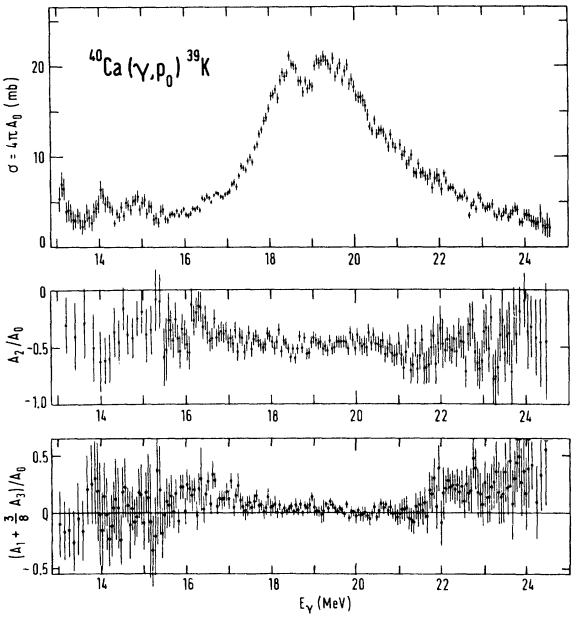

FIG. 4. Energy dependence of the cross section integrated over angles (upper diagram), and the corresponding Legendre polynomial coefficients (lower diagrams) for the ^{40}Ca$(\gamma, p_0)^{39}$K reaction in which the residual nucleus is left in the ground state.

We discuss below the origin of errors in the absolute cross-section scale arising from the normalization of the reduced yields and the shape of bremsstrahlung spectra:

i) Absolute calorimetric calibration of the Pruitt-type beam monitor is considered to be accurate within ±2%.[2] The error in the reproducibility of monitoring was negligible.

ii) The absolute number of irradiated nuclei in the target is subject to the ±2% inaccuracy of the target weight and to the ±2 – 4% inaccuracy in the measured distribution of the γ-ray beam over the target surface. This arises largely from the diffuse beam boundaries. There was no appreciable unflatness and inhomogeneity of the target. Moreover, the symmetrical mounting of detectors around the target annuls such errors for even Legendre polynomial coefficients and the calculated cross section would not be affected.

iii) The absolute values of the effective solid angles extended by detectors are estimated to

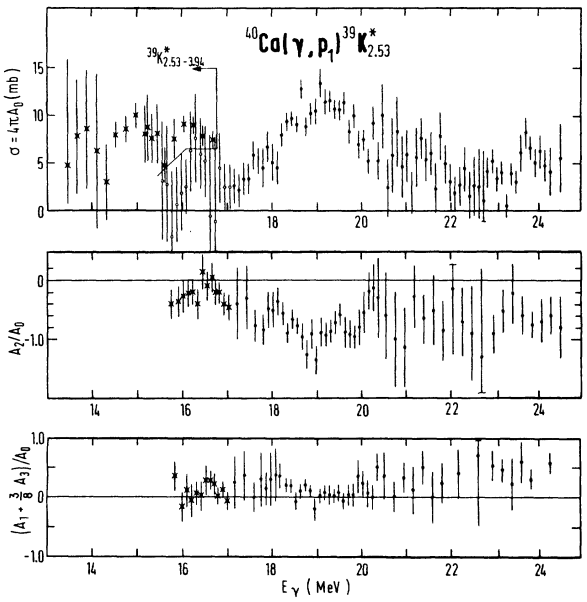

FIG. 5. Energy dependence of the cross section integrated over angles (upper diagram), and the corresponding Legendre polynomial coefficients (lower diagrams) for the ^{40}Ca$(\gamma, p_1)^{39}$K reaction in which the residual nucleus is left in the 2.53-MeV $\frac{1}{2}^+$ first excited state. Below E_γ =17 MeV separation of this state from higher neighboring states was possible only at 90°; therefore, at these energies angular distributions (crossed squares in the lower diagrams) were obtained from the sum of cross sections for levels between 2.53–3.94 MeV excitation energy (crossed squares in the upper diagram). Open circles below 17 MeV (upper diagram) represent the (γ, p_1) cross section evaluated from the 90° photoproton data and angular distributions of the summed cross sections.

TABLE I. Measured and calculated integrated cross sections for the main residual states. Present data are underlined.

Outgoing particles	Residual nucleus: Energy [MeV] and spin	Residual nucleus: Dominant shell-model hole configuration	Integrated cross sections up to E_γ [MeV mb]: Experiment (E_γ = 24.6 MeV): Deexcitation γ rays	Integrated cross sections up to E_γ [MeV mb]: Experiment (E_γ = 24.6 MeV): Photoprotons	Theory (E_γ = 25 MeV): Coupled-channel calculation with absorptive potential	Theory (E_γ = 25 MeV): Eigenchannel calculation without absorptive potential	Comparison of bremsstrahlung yields [a] at an end-point energy $E_{\gamma\max}$ [MeV mb]: Present meas. integrated over angles ($E_{\gamma\max}$ = 30.25 MeV)	Comparison of bremsstrahlung yields [a] at an end-point energy $E_{\gamma\max}$ [MeV mb]: Ullrich and Krauth (Ref. 55) ϑ = 120° ($E_{\gamma\max}$ = 32 MeV)
p_0	0 ; $\frac{3}{2}^+$	$(d_{3/2})^{-1}$		<u>100</u> ± <u>7</u>	255	350		
n_0	0 ; $\frac{3}{2}^+$			38 ± 4 [b]	90	110		
p_1	2.53; $\frac{1}{2}^+$	$(2s_{1/2})^{-1}$	<u>48</u> ± <u>6</u>	<u>49</u> ± <u>5</u> [c]	44 (12 [d])	190	<u>59</u> ± <u>4</u>	57
n_1	2.47; $\frac{1}{2}^+$		<u>16</u> ± <u>3</u>		11	30	<u>18</u> ± <u>2</u>	16
p	2.82; $\frac{7}{2}^-$		<u>11</u> ± <u>3</u>				<u>17</u> ± <u>2</u>	15
n	2.79; $\frac{7}{2}^-$		<u>2</u> ± <u>2</u> [e]				<u>3</u> ± <u>2</u>	
$p + (n)$ [f]	3.02; $\frac{3}{2}^-$		<u>14</u> ± <u>3</u>				<u>15</u> ± <u>2</u>	7
p	3.59; $\frac{9}{2}^-$		<u>2</u> ± <u>1</u> [e]	<u>45</u> ± <u>6</u> <u>50</u> ± <u>5</u> [c]			<u>2.3</u> ± <u>1.0</u>	
n	3.63; $\frac{9}{2}^-$							
$p + n$	3.88		<u>2.8</u> ± <u>0.8</u> [e]				<u>2.9</u> ± <u>0.7</u>	1.5
$p + (n)$ [f]	3.94		<u>11</u> ± <u>4</u>				<u>10.2</u> ± <u>1.5</u>	2.5
p	4.08		<u>3.6</u> ± <u>1.0</u> [e]				<u>3.5</u> ± <u>0.7</u>	
p	4.93		<u>5</u> ± <u>1</u> [e]				<u>5.4</u> ± <u>0.8</u>	2.0
n	5.13; $\frac{5}{2}^+$	$(d_{5/2})^{-1}$	<u>1</u> ± <u>1</u> [e]				<u>2.0</u> ± <u>0.7</u>	3.0
p	5.27; $\frac{5}{2}^+$		<u>8</u> ± <u>1</u> [e]				<u>6.5</u> ± <u>1</u>	3.8
p	5.31		<u>3.5</u> ± <u>1.5</u> [e]				<u>3.8</u> ± <u>0.6</u>	
n	5.48; $\frac{5}{2}^+$	$(d_{5/2})^{-1}$	<u>2</u> ± <u>1</u> [e]	<u>34</u> ± <u>6</u> <u>67</u> ± <u>8</u>			<u>2.2</u> ± <u>0.8</u>	
p	5.62; $\frac{5}{2}^+$		<u>9</u> ± <u>3</u> [e]				<u>8</u> ± <u>1</u>	1.6
p	5.83		<1 [e]		66	90	<u>2</u> ± <u>1</u>	
p	5.96		<1 [e]				<u>1</u> ± <u>1</u>	1.0
n	6.15; $\frac{5}{2}^+$	$(d_{5/2})^{-1}$	<u>2</u> ± <u>1</u> [e]				<u>1.5</u> ± <u>0.8</u>	0.9
p	6.35; $\frac{5}{2}^+$		<u>6</u> ± <u>1</u> [e]				<u>7</u> ± <u>1</u>	2.0
p_{unb}	6.5–8.0	$(d_{5/2})^{-1}$		<u>97</u> ± <u>15</u> [g]				
Total absorption			480 ± 40 [h]		470	780		
Total p			<u>363</u> ± <u>25</u>		365	630		
Total n			67 ± 4 [i] / 74 ± 7 [j]		110	150		

TABLE I (*Continued*)

[a] Listed yields are equal to the energy-integrated cross sections, assuming that they have shapes identical to the absorption cross section.
[b] Estimated from Ref. 20 assuming for the (γ,n_0) reaction the same angular distribution as for the (γ,p_0).
[c] In the region below $E_\gamma = 16$ MeV where (γ,p_1) could not be resolved, the integrated cross section for residual states between 2.53 and 4 MeV (amounting to 14 MeV mb) was assumed to be shared between (γ,p_1) and higher states in the same proportion as corresponding deexcitation γ-ray yields.
[d] The figure inside the brackets represents the part of integrated cross section in the region of the giant resonance.
[e] Because of low intensity, integrated cross sections are obtained by the method of Ref. (a).
[f] The contribution of neutron channel is negligible due to the high reaction threshold (see Fig. 11).
[g] The cross section for (γ,p_{unb}) has been extrapolated below $E_\gamma = 18.5$ MeV according to the shape of the transmission coefficients (extrapolated value of the cross section amounts to 23 ± 8 MeV mb).
[h] From Ref. 26.
[i] J. E. E. Baglin and B. M. Spicer, Nucl. Phys. 54, 549 (1964).
[j] B. S. Ishanov, I. M. Piskarev, I. M. Kapitonov, E. V. Lazutin, V. S. Sopov, and V. G. Shevchenko, Yad. Fiz. 13, 1141 (1971) [transl.: Sov. J. Nucl. Phys. 13, 655 (1971)].

TABLE II. Properties of residual-nuclei states and Legendre-coefficient ratios A_2/A_0 in the angular distributions of deexcitation γ rays to the ground states.

Energy of the excited residual state (MeV)		J^π	A_2/A_0 (Present experiment)	Mixing ratio for the decay to the $(\frac{3}{2})^+$ ground state
2.53	^{39}K	$\frac{1}{2}^+$	-0.04 ± 0.07	1 [a]
2.47	^{39}Ca	$\frac{1}{2}^+$	0.04 ± 0.13	1 [a]
2.82	^{39}K	$\frac{7}{2}^-$	-0.24 ± 0.14	-0.19 ± 0.10 [b] -0.12 ± 0.05 [c,d] -0.17 ± 0.04 [a]
3.02	^{39}K	$\frac{3}{2}^-$	-0.21 ± 0.12	0.03 ± 0.15 [b]
3.94	^{39}K (^{39}Ca)	$\frac{1}{2}$ or $\frac{5}{2}$	-0.32 ± 0.17	
4.93	^{39}K	?	0.06 ± 0.18	
5.27	^{39}K	$\frac{5}{2}^+$	0.23 ± 0.17	
5.62	^{39}K	$\frac{5}{2}^+$	0.19 ± 0.30	
6.35	^{39}K	$\frac{5}{2}^+$	0.31 ± 0.15	

[a] Reference 8.
[b] Reference 9.
[c] Reference 10.
[d] Reference 11.

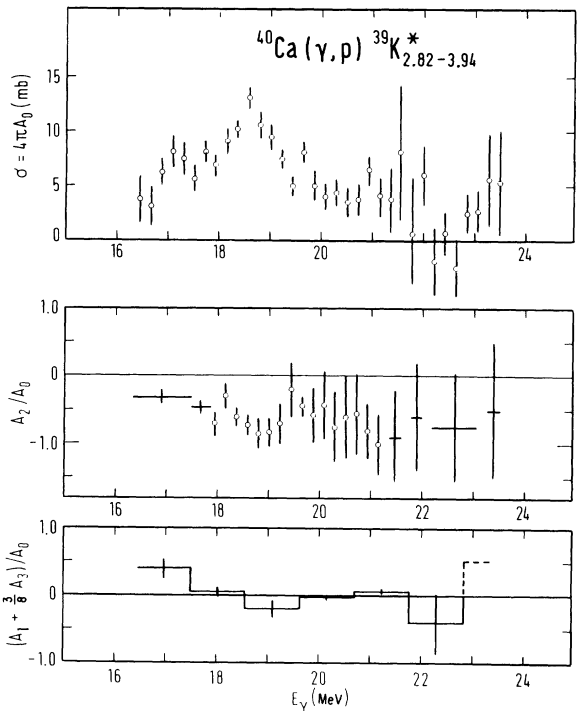

FIG. 6. Energy dependence of the cross section integrated over angles (upper diagram) and the corresponding Legendre polynomial coefficients (lower diagrams) for the ^{40}Ca$(\gamma,p)^{39}$K reaction populating states in ^{39}K between 2.82 and 3.94 MeV excitation energy. The main contribution is due to the levels 2.82 MeV $\frac{7}{2}^-$, 3.02 MeV $\frac{3}{2}^-$, and 3.94 MeV (see Fig. 3).

be accurate within ±2%.

iv) Experimentally determined bremsstrahlung spectra (Fig. 14) were used in the analysis. The effect of the corresponding errors in the absolute scale of the cross section is of the order of ±1%.

v) The energy calibration and the integral linearity of the detection system including multichannel analyzer are estimated to introduce an error of ±1%.

The last two sources of errors [(iv), (v)] also influence the shape of cross-section energy dependence. The comparison of results, obtained at different bremsstrahlung end-point energies and different amplifications, showed that the corresponding cross-section shapes agree within the statistical errors.

Assuming that the errors (i)–(v) are not correlated, the upper limit for the total systematic error of the absolute scale of the cross section, introduced through normalization of reduced yields and bremsstrahlung shape, is 6%. This error is

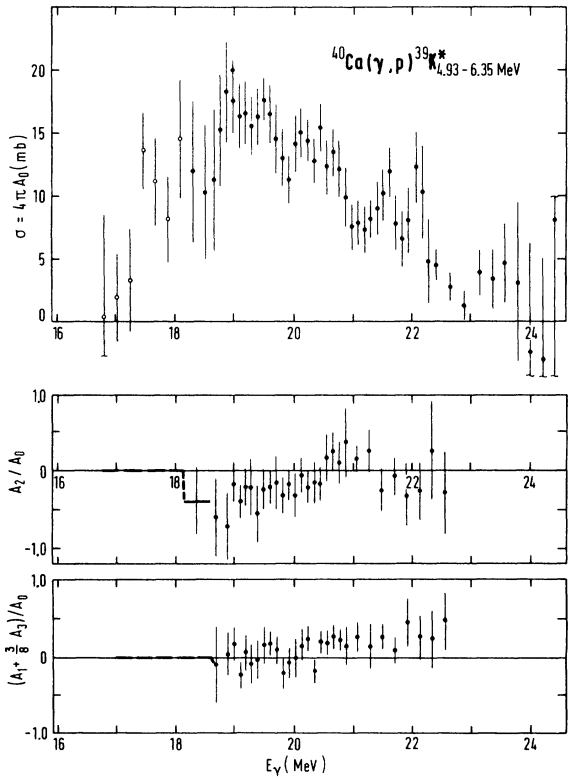

FIG. 7. Energy dependence of the cross section integrated over angles (upper diagram) and the corresponding Legendre polynomial coefficients (lower diagrams) for the ^{40}Ca$(\gamma,p)^{39}$K reaction in which states in the residual nucleus between 4.93 and 6.35 MeV excitation energy are populated. Below $E_\gamma = 18$ MeV the cross section was evaluated from the 90° photoproton spectra assuming isotropic angular distribution.

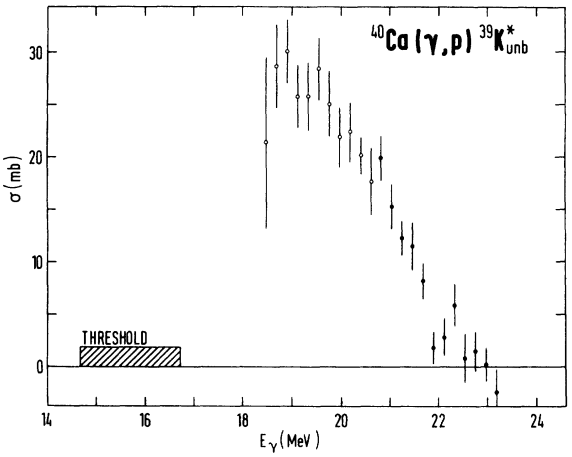

FIG. 8. Energy dependence of the cross section integrated over angles for the ^{40}Ca$(\gamma,p)^{39}$K reaction in which unbound states of residual nucleus are populated. In the least-squares analysis the contribution of all levels between 6.5 and 8.5 MeV was represented by a mean excitation energy of 7.4 MeV. Within errors, the angular distribution for photoprotons above $E_\gamma = 21$ MeV (closed circles) was isotropic, while below this energy isotropy was assumed and the cross section calculated from 90° photoproton data (open circles).

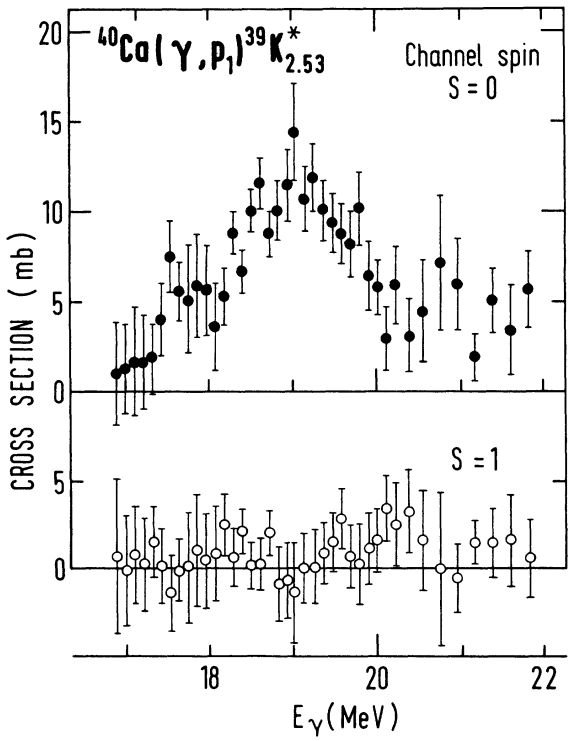

FIG. 9. Separated cross sections belonging to the channel spins $S=0$ (upper diagram) and $S=1$ (lower diagram) for the ^{40}Ca$(\gamma,p_1)^{39}$K reaction populating the 2.53-MeV $\frac{1}{2}^+$ first excited state in ^{39}K.

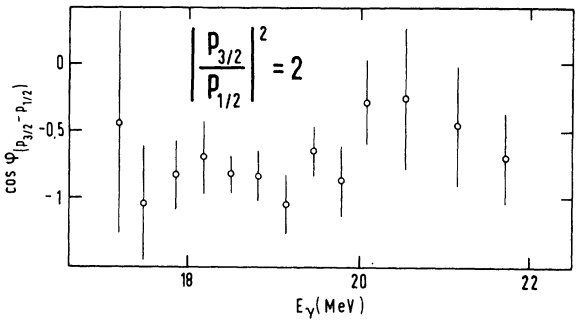

FIG. 10. Energy dependence of the relative phase angle between $p_{3/2}$ and $p_{1/2}$ proton waves in the ^{40}Ca(γ,p_1)-^{39}K reaction populating the 2.53-MeV $\frac{1}{2}^+$ first excited level in ^{39}K. A constant value of $\sqrt{2}$ was assumed for the $|p_{3/2}|/|p_{1/2}|$ amplitude ratio.

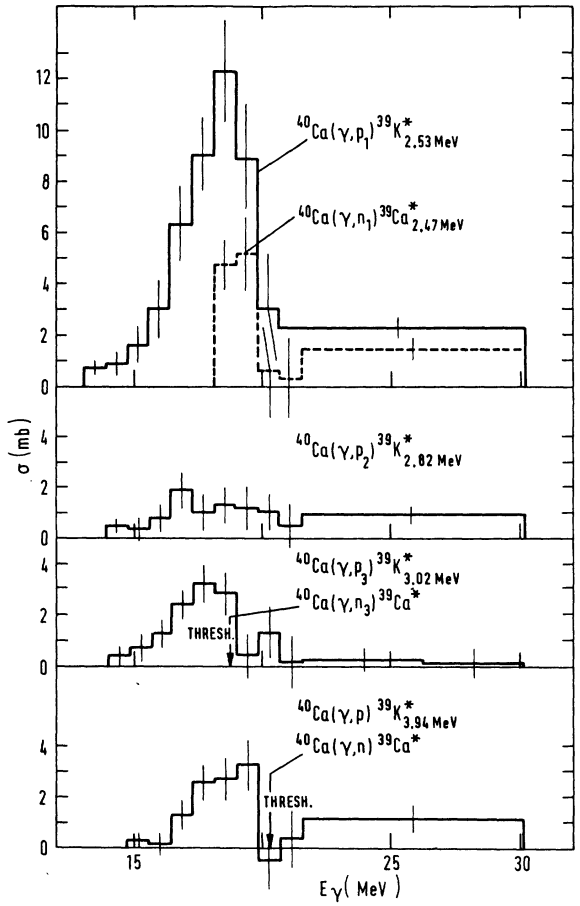

FIG. 11. Cross sections for reactions (γ,p) and (γ,n) in ^{40}Ca calculated by the matrix inversion method (Ref. 7) from the yields of the strongest γ lines in deexcitation spectra. The yields were corrected for cascades from known decay schemes and those observed in deexcitation spectra. Vertical bars on histograms represent statistical errors.

not shown explicitly in the diagrams, however, it is practically the only error [exclusive of error (v)] quoted for the energy-integrated cross sections in Table I (where the statistical error and/or errors introduced through least-squares fit are much smaller). The error bars plotted on diagrams of Figs. 4–10 represent either true statistical errors of measured yields, or errors calculated from the χ^2 analysis; for each data point the larger of the two was adopted. The statistical errors were larger than χ^2 errors in about $\frac{2}{3}$ of the cases. Therefore, it is reasonable to expect that errors from numerical analysis do not contribute significantly to the plotted

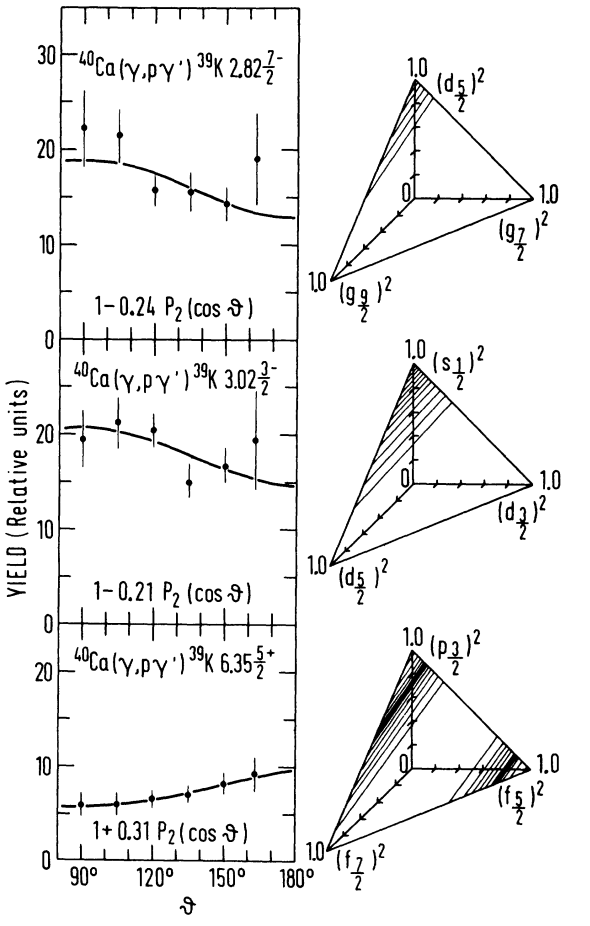

FIG. 12. Angular distributions of deexcitation γ rays from the 2.82-MeV $\frac{7}{2}^-$, 3.02-MeV $\frac{3}{2}^-$, and 6.35-MeV $\frac{5}{2}^+$ levels in ^{39}K measured at 30.25-MeV bremsstrahlung end-point energy. The solid curves are fits to Legendre polynomial expansions $1+(A_2/A_0)P_2(\cos\vartheta)$. Configurations of reaction channels are shown on phase-space diagrams (right half of the figure), where the squares of amplitudes are represented as rectangular coordinates of a point on the surface of the plane. The shading density shown represents the precision of the experimentally determined configuration.

errors. In connection with the choice of mean energies to represent the position of groups of levels unresolved by the least-squares fit (Figs. 6–8), trial calculations have been made and show that small changes around the chosen values do not appreciably affect the magnitude of the cross sections.

The accuracy of the ratios of Legendre polynomial coefficients is affected by two kinds of systematic errors only: errors in the determined ratio of effective detector solid angles (which was known within ±1.5%), and irregularities and improper mounting of the target itself (which could affect the odd coefficients only). The yield ratio of the two detectors placed symmetrically on either side of the target at an angle close to 90° did not reveal any errors of the latter type. We conclude, therefore, that statistical errors or χ^2 errors shown in diagrams are by far the largest appearing in the angular distributions.

The yields of the intense lines in the spectra of deexcitation γ rays have been analyzed by the inverse matrix method of Penfold and Leiss[7] and the errors resulting from analysis are less than the statistical errors in our measurements.

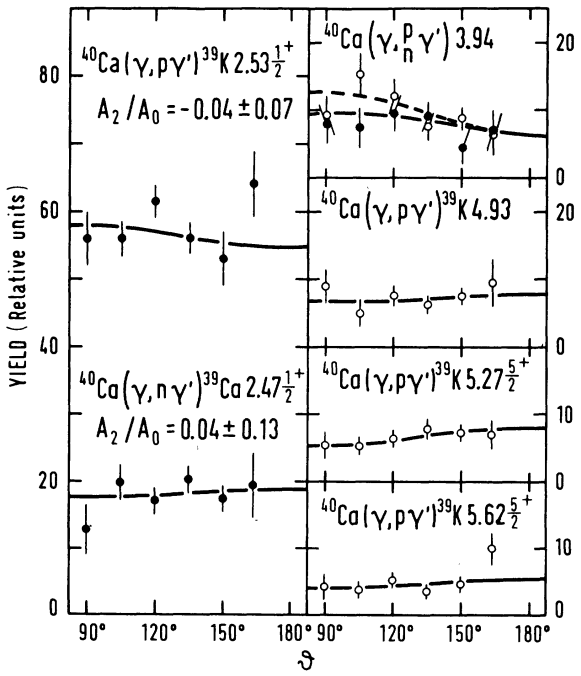

FIG. 13. Angular distributions of deexcitation γ rays from several excited states in ^{39}K and ^{39}Ca listed in Table II. Open and closed circles represent data obtained from full-energy and double escape peaks, respectively. The solid curve is a fit to the Legendre polynomial expansion $1+(A_2/A_0)\,P_2(\cos\vartheta)$.

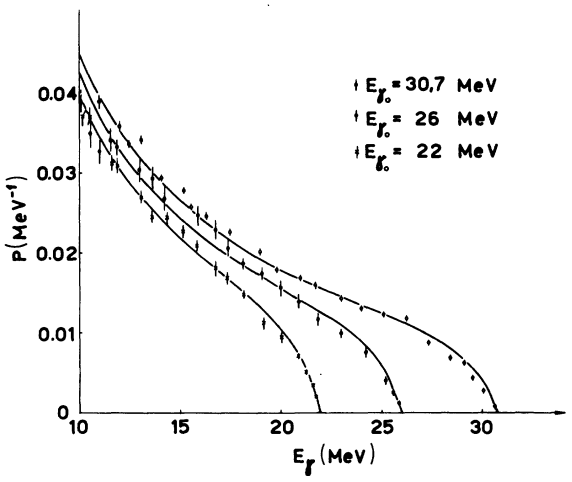

FIG. 14. Shapes of the γ-ray bremsstrahlung spectra obtained by Compton-spectrometer measurements and used for cross-section calculations in the present work. Spectra calculated from Schiff's formula integrated over angles are shown for comparison (solid curves).

Systematic errors of the absolute scale of the cross section introduced by the sources discussed in paragraphs (i)–(v) are estimated to amount up to ±6%. Additional sources of systematic errors can, however, be introduced into these measurements by cascading γ rays, especially since the decay scheme of ^{39}K for the levels above 5 MeV is not known. The corresponding corrections for the yields of the low-lying levels were performed on the basis of the known decay schemes. It was assumed that the states above 5 MeV decay only

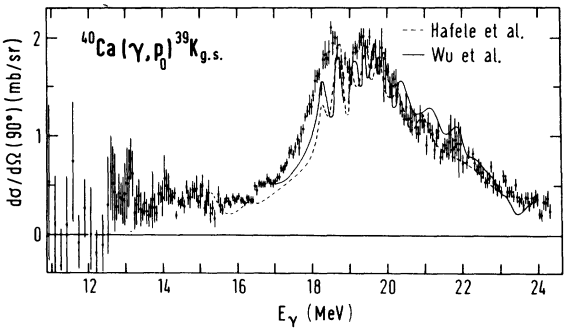

FIG. 15. Comparisons of differential cross sections for the $^{40}Ca(\gamma,p_0)^{39}K_{g.s.}$ reaction at 90°: present work (points with error bars), the data of Wu *et al.* (Ref. 20) (full curve), data from the inverse reaction of Hafele, Bingham, and Allen (Ref. 16) (dashed curve). The solid and dashed curves have been arbitrarily drawn through the experimental points. Errors in the absolute cross-section scale determination are ± 6% for the present work, ± 10% for Ref. 20, and ± 70% for Ref. 16.

to the ground state, with the exception of the 5.62-MeV state, for which the 2.61-MeV line was ascribed to the 5.62 → 3.02-MeV cascade. It is possible that some cascade lines with energies less than 1 MeV were hidden in heavy background at low energies and were unobserved. The magnitude of this type of errors is difficult to estimate. Nevertheless, the comparison of integrated deexcitation cross sections to proton cross sections shows that errors of this type are not large.

IV. DISCUSSION

A. (γ,p_0) reaction

Previous experimental data on the (γ, p_0) reaction[14-22] consist mainly of differential cross sections at one angle only (with the exception of Ref. 21 where measurements at two angles are presented for the low-energy part), while angular distributions were not studied extensively. Therefore, in the present work only 90° data are compared to other experimental results. In Fig. 15 we see that present measurements reproduce well the cross-section shape of Refs. 16 and 20 except for the possible energy shift of ≈150 keV. Such good agreement is also found with low-energy data of Refs. 19 and 21 (peaks at 12.6, 13.1, and ≈ 14 MeV) for which no energy shift is observed also. Wu *et al.*[20] (Fig. 15) measured the (γ, p_0) cross section in the γ-ray energy interval 17–24 MeV and determined its absolute value within an error of 10% which is comparable to the 6% precision of the present work and the experiments agree on the same magnitude of the cross section. On the other hand, little significance can be attached to the agreement with absolute value of the other experiments in which data are obtained with lower precision. It should be noted that Feldman, Baliga, and Nessin[17] present for the (p, γ_0) cross section (not shown in Fig. 15) an absolute value which amounts to only about half the value observed in the other experiments. However, these authors obtain a similar discrepancy for the reaction ^{11}B$(p, \gamma_0)^{12}$C (cf. Refs. 23–25).

The cross section integrated over angles (Fig. 4) shows essentially the same structure as the 90° data. Its shape is in good agreement with the total photonuclear cross section.[26]

The existing continuum theory calculations[27,28] are based on pure shell-model configurations for the ^{40}Ca ground state and the states of residual nuclei. Therefore the significance of the comparison with theoretical results depends on the purity of these states. It has been argued on the bases of experimental[29-31] and theoretical[32-35] work that the ground state of ^{40}Ca contains, besides its dominant closed shell structure, considerable admixture (about 30%) of more complicated states also (some authors[36-39] suggest even larger impurities). Similarly, there seem to be indications[40,41] for the presence of core excitations in the dominantly $d_{3/2}$ hole ground-state wave function of ^{39}K.

Cross sections for the $d_{3/2}$ reaction channels resulting from 1p-1h coupled channel[27] and eigenchannel[28] calculations based on Woods-Saxon potential greatly exceed the measured value for the (γ, p_0) reaction. The introduction of an absorptive potential[27] tends to reduce the cross section and to broaden the peaks, thus partly diminishing the discrepancy with the experimentally observed gross structure. The calculated cross section of Marangoni and Saruis[27] (Fig. 16) is in a fair agreement with the experimental results as far as the energy distribution of the (γ, p_0) width is concerned, while in other cases including bound state calculations (cf. Refs. 36, 42) too low energies are obtained for the position of the main peaks.

The experimental integrated (γ, p_0) cross section up to a γ-ray energy of 25 MeV amounts to $21 \pm 3\%$ of the giant resonance photoabsorption cross section (Table III), as compared to the calculated continuum theory values for the $d_{3/2}$ hole channels of 45%[28] and 53% (with an absorptive potential in the latter case).[27] On the other hand, Gillet and Sanderson[36,42] obtain in their bound-state calculation 24% for the $d_{3/2}$ hole contribution to the total dipole strength. Since the (γ, p_0) integrated cross section is 2.2 times larger than the (γ, n_0) cross section,[20] the amount of $d_{3/2}$ hole strength that should be attributed to the proton channel following the results of Gillet and Sanderson is 17%, in good agreement with the observed value for the ground-state cross section. All these authors use pure shell-model ground-state configurations in their calculations.

In previous experiments only angular distributions at a few values of proton energies were measured[22] and in some cases[14,18] a bremsstrahlung-weighted angular distribution was presented. The ratio of Legendre polynomial coefficients A_2/A_0 from these experiments ranges from −0.3 to −0.5 which, considering their experimental uncertainty, is in good agreement with the present average value of −0.45. The only serious discrepancy seems to arise at an excitation energy of 14 MeV, where Diener *et al.*[22] present a value of 0.6 ± 0.2, excitation functions of Heimlich and Mausberg[21] at 0 and 90° imply $A_2/A_0 \approx 0.2$, while present data (Fig. 4) give a value around −0.5. There seems to be no explanation for such a disagreement.

Although the number of measured Legendre polynomial coefficients is smaller than the number of unknown parameters in angular distributions,

one can still use them for a restriction of possible reaction channel configurations. Assuming only $E1$ transitions to continuum states of ^{40}Ca, a pure $f_{5/2}$ configuration would give $A_2/A_0 = -0.40$ (see, e.g., formulas in Ref. 43), while only a small admixture ($\frac{1}{2}\%$) of $p_{1/2}$ proton waves would suffice to fit the experimentally observed mean value of -0.45. Of course, larger admixtures of $p_{1/2}$ (up to 90%) are also consistent with the present data. This is compared to the prediction of Gillet and Sanderson[36,42] for the composition of the main dipole state at 18 MeV which gives 6% for $|p_{1/2}|^2$ (with a negligible spin-flip $p_{3/2}$ amplitude).

Similarly, as observed with other nuclei, the coefficients A_2/A_0 of photoproton angular distributions are fairly energy-independent. This is in contradiction to continuum theory calculations (cf. Fig. 17) where large variations are predicted. There is a slight correlation between the experimental data and the theory[27] in the vicinity of 16.5 MeV, where measured A_2/A_0 coefficients have smaller absolute values although they are still negative (calculation predicts positive values but their magnitude and sign are very sensitive to

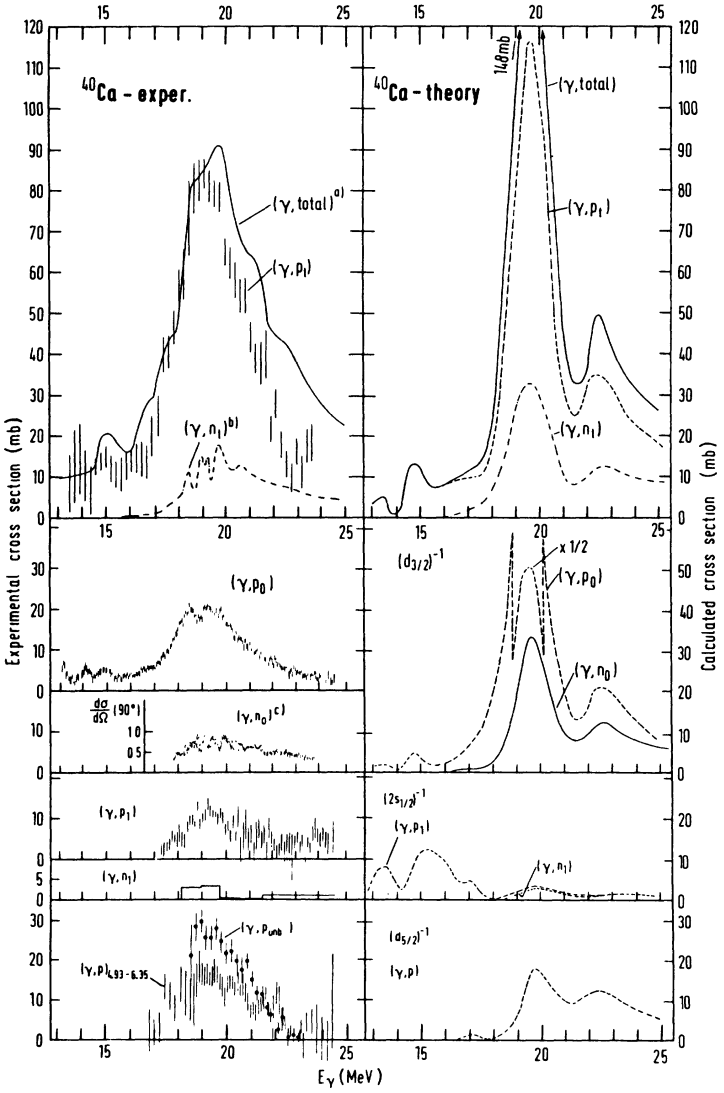

FIG. 16. Comparisons of experimental results (left half of the figure) to the theoretical $1p$-$1h$ coupled-channel calculations with absorptive potential of Marangoni and Sarius (Ref. 27) (right half of the figure). Beside present results (unlabeled), the following data are presented on the left half of the figure: (a) total absorption cross section from Ref. 26; (b) (γ, n_t) total cross section from Table I, Ref. (i); (c) (γ, n_0) differential cross section from Ref. 20 where the absolute scale representing the cross section integrated over angles was plotted assuming the same angular distributions as obtained from the (γ, p_0) reaction in the present work.

relative phases of continuum state eigenvectors). Consistently with the prediction of Marangoni and Saruis,[27] this might be due to the presence of a larger proportion of the $p_{1/2}(d_{3/2})^{-1}$ amplitude in this energy region.

B. (γ,p_1) and (γ,n_1) reactions

The cross sections for the (γ, p_1) reaction integrated over angles obtained from the measurement of protons and deexcitation γ rays (see Figs. 5 and 11, respectively) agree with each other within the experimental errors.

It is noted that the energy dependence of the cross section has a gross structure similar to the total photoabsorption cross section (cf. Fig. 16) and peaks at the same photon energy. This feature—already observed in (γ, p_0)—seems to be typical for all partial cross sections. It is in contradiction to the expectations from the coupled channel calculation of Marangoni and Saruis[27] where no peaking at 19 MeV is predicted (Fig. 16) for the (γ, p_1) cross section. On the other hand, Barrett *et al.*[28] present a result of eigenchannel calculation in which the (γ, p_1) cross-section peaks at 17 MeV, as does their predicted nuclear photoabsorption cross section. Their results, however, indicate a 5-MeV displacement towards higher energies for the peak of the (γ, n_1) cross section which is not observed experimentally (Figs. 11 and 16). The (γ, n_1) cross section is about 3 times smaller than (γ, p_1). The isospin impurity of the giant dipole state can be estimated using the expression of Barker and Mann.[44] A value between 0–0.18 is found[45] for the ratio of the $T=0$ to $T=1$ amplitude, in agreement with a similar value

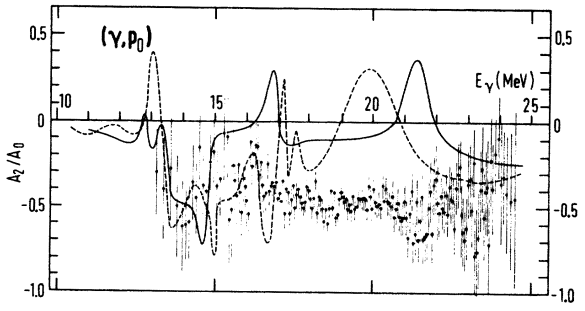

FIG. 17. Measured ratio of Legendre polynomial coefficients A_2/A_0 from the ^{40}Ca$(\gamma, p_0)^{39}$K$_{g.s.}$ reaction, compared to predictions of coupled-channel calculation (Ref. 27) (solid curve) and eigenchannel calculation (Ref. 28) (dashed curve) for the $(d_{3/2})^{-1}$ reaction channel.

obtained for the ground-state cross sections. Both cross sections (γ, p_1) and (γ, n_1) together comprise 14% of the nuclear absorption cross section, which is fairly consistent with the value of 9% for the $2s_{1/2}$ hole configuration obtained by Gillet and Sanderson[42] in their bound-state calculation (Table III). The agreement with continuum calculations is less satisfactory. The predicted proportion for the $(\gamma, p_1 + n_1)$ cross section in the giant dipole region is 4.5% (coupled channel[27]) and 28% (eigenchannel[28]) of the total photonuclear cross section. In the former case this discrepancy and the displacement of the cross section peak are possibly due to a different choice of the $p_{3/2}$ single particle energy (0.5 MeV lower). In the latter case the excessive (γ, p_1) cross section is probably of a more general character.

TABLE III. Measured and calculated main decay modes of GDR in ^{40}Ca. Present results are underlined.

Reaction	Residual nucleus: Energy and spin of the residual state	Residual nucleus: Dominant shell-model hole config.	Integrated cross sections relative to the integrated total absorption cross section (%): Experiment	Coupled-channel calculation[a]	Eigenchannel calculation[b]	Bound state calculation[c]
(γ,p_0)	0 MeV; $\frac{3}{2}^+$, ^{39}K	$(d_{3/2})^{-1}$	<u>21</u>	53	45	24
(γ,n_0)	0 MeV; $\frac{3}{2}^+$, ^{39}Ca		<u>8</u>[d]	20	14	
(γ,p_1)	2.53; $\frac{1}{2}^+$, ^{39}K	$(2s_{1/2})^{-1}$	<u>10.5</u>	9 (2.5[e])	25	9
(γ,n_1)	2.47; $\frac{1}{2}^+$, ^{39}Ca		<u>3.5</u>	2	4	
(γ,p)	2.82–4.08, ^{39}K		<u>10.5</u>			
(γ,p)	4.93–8.0, ^{39}K	$(d_{5/2})^{-1}$	<u>34</u>[f]	14	11	67
(γ,n)	5.11–6.13; $\frac{5}{2}^+$, ^{39}Ca		<u>2</u>	2	1	

[a] Reference 27. Theoretical integrated total absorption cross section is a sum of the 1p-1h reaction-channel cross sections calculated with absorptive potential.

[b] Reference 28.

[c] References 36, 42.

[d] Reference 20, assuming angular distribution of (γ,p_0) as obtained in the present work.

[e] The figure in parentheses represents the part of integrated cross section in the region of the giant resonance.

[f] ^{40}Ca$(\gamma,p)^{39}$K$_{>4.93}$.

The analysis of the (γ, p_1) cross section in terms of channel spin representation shows an interesting feature. Only channel spin 0 exhibits a resonant behavior, while $S=1$ cross section is remarkably nonresonant (Fig. 9). The dominance of the $S=0$ amplitude is consistent with the picture according to which the dipole operator affects mainly the space part of the wave function of the nucleus. We only note that in the $^{31}P(p,\gamma_0)^{32}S$ reaction[4] the fluctuation analysis gave no indication for different reaction mechanisms since similar proportions of direct components were found in both channels. As in the case of $^{31}P(p,\gamma_0)^{32}S$ the $S=0$ channel is dominant also in the $^{40}Ca(\gamma,p_1)$ reaction.

For the comparison with theory an analysis in the j-j coupling scheme is more convenient although it is somewhat ambiguous. It was performed with the assumption of a constant amplitude ratio $|p_{3/2}|/|p_{1/2}| = \sqrt{2}$. Such an amplitude ratio is consistent with all A_2/A_0 values encountered in the (γ, p_1) angular distributions, as well as with the dominance of the channel spin $S=0$ strength. It also agrees with the ratio of $(2s_{1/2})^{-1}(1p_{3/2})$ and $(2s_{1/2})^{-1}(1p_{1/2})$ amplitudes predicted by Gillet and Sanderson[42,36] (the 18.6-MeV state in the latter case). The resulting phases shown in Fig. 10 are rather insensitive to changes of amplitude ratio. The average value of the phase angle between the $|p_{1/2}|$ and $-|p_{3/2}|$ amplitudes is about 50°. It shows considerable variations in the region of the giant resonance peak. Similar variations of the phase angle between the $s_{1/2}$ and $d_{3/2}$ amplitudes were observed in the $^{15}N(p,\gamma_0)^{16}O$ reaction.[5]

C. Photonuclear reactions to channels involving negative-parity states of residual nuclei

The negative-parity states of the residual nuclei are mainly populated through the photoproton reactions. The dominant contribution—amounting to 7% of the photonuclear absorption cross section in the giant resonance region—comes from the states at 2.82 MeV ($\frac{7}{2}^-$) and 3.02 MeV($\frac{3}{2}^-$) in ^{39}K. The ^{39}K 3.94-MeV state, for which the spin and parity are uncertain,[46,47] contributes about 2% to the total photonuclear cross section. The results of the matrix inversion method applied to the deexcitation γ-ray spectra are shown in Fig. 11 in the form of energy-dependent cross sections. Photoproton spectra, on the other hand, provide summed (γ, p) cross sections for the states of the residual nucleus ^{39}K in the energy region 2.82 –3.94 MeV (Fig. 6). The latter compares well with the deexcitation results for the sum of contributions to states at 2.82, 3.02, and 3.94 MeV. The small difference can be accounted for by the reaction channels involving states at 3.59, 3.88, 4.08, and possibly at 4.02 MeV (unobserved). These states have not been considered in the above sum.

Negative-parity states are considerably less populated in the (γ, n) reaction. The yield to the 2.80-MeV state in ^{39}Ca is only about 0.2 times the yield of its (γ, p) counterpart (the $\frac{7}{2}^-$ 2.82-MeV state in ^{39}K). The yield to this state was too small to allow a deduction of the energy dependence for the cross section. Even smaller is the contribution of the $\frac{3}{2}^-$ 3.03-MeV state due to the prohibitive reaction threshold (19 MeV). It could not be resolved in the deexcitation spectra because of the proximity of γ rays from the analogous state in ^{39}K.

The limits for the proton wave amplitudes have been deduced from the angular distributions of the deexcitation γ rays. The spin-flip amplitudes are small, and while $d_{5/2}$ (for the 2.82-MeV state) and $s_{1/2}$ (for the 3.02-MeV state) amplitudes seem to dominate, admixtures of up to 60% of $|g_{9/2}|^2$ and 70% of $|d_{5/2}|^2$, respectively, would still be consistent with the deexcitation data. A further restriction is imposed by proton angular distributions; a simultaneous absence of $d_{5/2}$ (for the 2.82-MeV state) and $s_{1/2}$ (for the 3.02-MeV state) proton waves would be inconsistent with the large negative A_2/A_0 value (Fig. 6).

Theoretical predictions for negative-parity hole channels would have to take into account configuration mixing in the ground state and/or second-order reaction processes. Such calculations have not yet been performed. Nevertheless, it is tempting to try to understand the mechanism leading to such photonuclear reaction channels. There is evidence for the admixture of a considerable amount of $[(1d_{3/2})^{-2}(1f_{7/2})^2]_{J=0^+}$ configuration in the ground state of ^{40}Ca.[29,35,9,48,49] A γ-ray excitation of this configuration could result in a dipole state formed by $[(1d_{3/2})^{-2}(1f_{7/2})]_{7/2^-}$ coupled to either a $d_{5/2}$, $g_{7/2}$, or $g_{9/2}$ particle. The above configuration (two $d_{3/2}$ holes in a doubly closed $2s1d$ shell and one $f_{7/2}$ particle) is just the one which seems to be dominant[50,51] in the $\frac{7}{2}^-$ 2.82-MeV state of ^{39}K. It will be shown later that an alternative mechanism is also possible.

A similar interpretation for the $\frac{3}{2}^-$ contribution is less appropriate since the population of this state in the pickup reactions is about an order of magnitude smaller, while the integrated photonuclear cross section for the corresponding channel is about the same magnitude. Furthermore, there are indications that the 3.02-MeV $\frac{3}{2}^-$ state could be described as a collective state[51,52] either by phonon-hole interaction[53] or by weak coupling of the ^{40}Ca excited core (the 3^- vibrational state

at 3.73 MeV) to a $d_{3/2}$ hole.[54] In both cases the dominant configurations of the $\frac{3}{2}^-$ state in ^{39}K are similar. The photonuclear reaction through this channel could be understood as a two-step process. In the first step the absorbed γ ray excites a proton to the $f_{5/2}$ shell (as already noted, excitations $2p_{1/2}$ and $2p_{3/2}$ contribute little to the $d_{3/2}$ hole configuration). In the second step this proton inelastically scatters on the ^{39}K core, exciting it to the $\frac{3}{2}^-$ state. Such an interpretation implies that the shape of the ^{40}Ca$(\gamma, p)^{39}$K$_{3.02}$ cross section should be correlated to the one for ^{40}Ca$(\gamma, p)^{39}$K$_{g.s.}$. This is not in disagreement with present observations (Fig. 11).

A two-step reaction process could provide an alternative mechanism also for the photonuclear process leading to the 2.82-MeV hole channel, especially since the yield in the (p, p') scattering on ^{39}K is relatively large[9] and there is evidence[47] for a significant admixture of collective configurations in the 2.82 MeV ^{39}K state. Keeping in mind the magnitude of the spectroscopic factor for this state, it is most likely that both configuration mixing in the ground state [combined with a direct (γ, p) reaction] and a two-step process are responsible for the observed yield in this reaction channel.

All the above conclusions are based on the assumption that the photonuclear processes involve mainly $E1$ transitions. This assumption is justified by the almost nonexistent odd Legendre polynomial coefficients in the angular distributions of protons.

The interpretation of the data for the 3.94-MeV state in ^{39}K is presently not possible due to the unknown properties of this state.

D. Reaction channels involving excitations of residual nuclei above 4.93 MeV

Photonuclear reactions in which residual nuclei are left in excitations of 4.93 MeV or more are almost entirely limited to proton channels because of high thresholds for other processes. The (γ, p) cross section is roughly equally divided between channels with the nucleus ^{39}K in its bound and unbound (excitations above 6.35 MeV) states (Fig. 16).

As for all of the rest of the channels with ^{39}K and ^{39}Ca in excited states, the only other existing experimental data are those of Ullrich and Krauth[55] consisting of deexcitation γ-ray yields. Their results show a systematic relative decrease of yields with increasing energy as compared to the presently measured integrated cross sections (Table I). Such an effect could be due to an error in the determination of the efficiency function of the Ge(Li) detector.

The integrated cross section from deexcitation data in this energy region (assuming an uniform giant resonance shape for all partial cross sections) accounts for about 55% of the bound-state integrated cross sections seen in the photoproton experiment (Table III). The remaining yield is unobserved probably due to the large number of residual states which are poorly populated in photonuclear reactions. These residual states decay either directly to the ground state or through intermediate states. The only cascade observed in the present work is the decay 5.62 MeV $(\frac{5}{2}^+)$ $\rightarrow$ 3.02 MeV $(\frac{3}{2}^-) \rightarrow$ g.s. $(\frac{3}{2}^+)$, presumably with a branching ratio[56] of about 0.5. In this energy region mainly $\frac{5}{2}^+$ bound states of ^{39}K are populated (the three $\frac{5}{2}^+$ states at 5.27, 5.62, and 6.35 MeV account for about 60% of the cross section seen in the deexcitation spectra). It is typical that the extent of population of these states is roughly proportional to the spectroscopic factors found in nucleon transfer reactions[29] which also seem to have a dominant $d_{5/2}$ configuration. It is believed that the $d_{5/2}$ hole configuration may extend to excitations in the continuum as high as 8 MeV or more,[57] with a center of gravity at about 6.6 MeV. Therefore it is justified to assume that the reaction channels involving states of ^{39}K with excitations above 4.93 MeV have a dominant $d_{5/2}$ hole configuration.

The energy integral up to 24.6 MeV excitation in ^{40}Ca yields a value of 163 MeV mb for the photoproton cross section involving states in ^{39}K above 4.93 MeV (Table I). It corresponds to 34% of the total absorption cross section[26] in the same energy region. This result is compared to calculated values of 13% for the $d_{5/2}$ hole channels, obtained using continuum theories.[27,28] On the other hand, the bound-state calculation of Gillet and Sanderson[36] predicts a $d_{5/2}$ hole contribution to the giant resonance state of as much as 66%. It was shown by Fujii[58] for the case of shell-model continuum calculations that the branching of the dipole resonance into different reaction channels depends critically on the parameters of the two-body interaction. It is probable, therefore, that a suitable choice of the two-body interaction potential would improve the agreement between the experimental data and the results of continuum calculations, as far as the branching is concerned.

The shape of the ^{40}Ca$(\gamma, p)^{39}$K$^*_{>4.93\ \mathrm{MeV}}$ cross section follows the general pattern of the ^{40}Ca giant dipole resonance with the exception of the low-energy part which is depressed due to the vicinity of reaction thresholds. The shape also shows a general agreement with the results of the coupled channel calculation[27] except for the 1-MeV shift. The ^{40}Ca$(\gamma, p)^{39}$K$^*_{4.93-6.35}$ part of the cross section

exhibits some structure in the energy region around 22 MeV, which might correspond to the peak at 22.4 MeV in the data of Marangoni and Saruis. The configuration of the wave function for this peak involves $f_{5/2}(d_{5/2})^{-1}$ and $f_{5/2}(d_{3/2})^{-1}$ components. Thus dominantly $f_{5/2}$ proton waves would be expected. The same configuration is also predicted by Gillet and Sanderson at a somewhat lower energy. A pure spin-flip amplitude would produce a positive value for the A_2 coefficient in angular distributions. Unfortunately, very small admixtures of other waves may change the A_2 value considerably. At energies above 20.5 MeV there seems to be a tendency for angular distributions to change from a negative A_2 value to almost zero (Fig. 7), which might be due to a dominant spin-flip amplitude in this region.

Neither angular distributions of deexcitation γ rays for the ^{39}K states at 5.27, 5.62, and 6.35 MeV nor angular distribution of protons to the 4.93–6.35-MeV ^{39}K bound states can lead to a detailed determination of the proton channel configuration. This is seen from the experimental values for A_2/A_0 coefficients and the formulas for angular distributions.[13,43] Both types of angular distributions favor dominant $p_{3/2}$ proton waves, but a reaction channel configuration identical with the theoretically predicted[36,42] $d_{5/2}$ hole configuration of dominant $f_{7/2}$ particles in the dipole state would still be consistent with the experimental data. It is, however, reasonable to assume that the dipole state configuration and the reaction channel configuration are not identical because of the different transmission coefficients for p and f waves. Therefore, we expect the proton p-wave amplitude to be enhanced as indicated by the experimental results.

The experimental uncertainties of the channel amplitudes are mainly due to the unknown mixing ratios for the decay of the $\frac{5}{2}^+$ states. As seen from the formulas for the deexcitation γ rays, present experimental results restrict the possible values of the mixing ratio for the 6.35-MeV state to $\delta<0$ or $\delta>0.45$ (here the phase convention of Rose and Brink[13] was used).

The small value of odd Legendre polynomial coefficients in angular distribution of protons indicates that most of the cross section is due to reaction channels involving $J^\pi = 1^-$ intermediate states in ^{40}Ca, as assumed in the analysis.

V. CONCLUSIONS

The presented experimental data comprise cross sections and angular distributions for most of the photoproton and photoneutron reaction channels. Cross sections for photonuclear channels studied in the present work, to which the (γ, n_0) cross section[20] is added (a contribution of about 8%), represent $90 \pm 10\%$ of the total photoabsorption cross section of Ref. 26. The measurement of photoprotons and deexcitation γ rays provided a double set of experimental results which are consistent with each other. The present result for the case of the (γ, p_0) differential cross section, which was also measured elsewhere, is in a complete agreement with these data.

It is shown that less than $\frac{1}{3}$ of the photonuclear absorption cross section is due to reaction channels with the residual nuclei in their ground states, while results of continuum theory calculations ascribe $\frac{2}{3}$ of the cross section to the ground-state transitions. On the other hand, there seems to be a consistency between the configuration of the dipole state in the bound-state calculation of Gillet and Sanderson and the experimentally found information about the reaction channel configurations. This is exhibited in the experimental data in two ways. Firstly, the branching of the giant resonance into channels with different hole configurations (observed through the integrated cross sections for processes involving residual nuclei in different states) is in agreement with the predicted hole configurations of the giant dipole state. Secondly, angular distributions of protons and deexcitation γ rays indicate dominant $f_{5/2}$ waves in (γ, p_0), $p_{3/2}$ waves in (γ, p_1) and p waves for reaction channels in which mainly $\frac{5}{2}^+$ states are populated (excitations above 4.93 MeV). This is again consistent with the predictions of Gillet and Sanderson.

All the measured partial reactions exhibit similar resonant energy dependence, with the cross sections peaking at the same energy of about 19 MeV. Such a uniformity of the cross sections is not in a good agreement with results of coupled-channel and eigenchannel calculations.

Theoretically predicted variations of angular distributions are likewise not found experimentally. The weak energy dependence of angular distributions which was observed elsewhere in other nuclei is also found here. In two cases, however, there are indications for a correlation between theoretical results of Marangoni and Saruis, and the experimentally found angular distributions. These are: the (γ, p_0) reaction in the vicinity of $E_\gamma = 16.5$ MeV with a predicted $p_{1/2}(d_{3/2})^{-1}$ dominant configuration, and the photoproton reactions involving residual nuclei states with excitations above 4.93 MeV where a $f_{5/2}(d_{5/2})^{-1}$ configuration is predicted.

Angular distributions are slightly forward peaked with odd Legendre polynomial coefficient close to zero for all proton channels. This indicates small

admixtures of even electromagnetic multipolarity terms.

The separation of the (γ, p_1) cross section into two channel spin contributions shows that only the dominant $S=0$ part of the cross section has a resonant structure, while $S=1$ is almost energy-independent. This interesting phenomenon may still need an explanation and further investigation.

In negative-parity channels—for which no theoretical predictions exist—proton waves with lowest possible l values seem to dominate. It is proposed that such reaction channels are connected to the existence of two-step reaction processes and impurities in the ground state of ^{40}Ca.

The ratio of (γ, p_1) and (γ, n_1) cross sections of 2.5 implies an $T=0$ to $T=1$ amplitude ratio in the ^{40}Ca giant resonance of about 0.1. It is shown that this is in agreement with the results obtained for the ground-state transition if the ratio of transmission coefficients is taken into account.

Finally, it is demonstrated on the 6.35 MeV $\frac{5}{2}^+$ state that in some cases photonuclear reactions can be useful in the study of spectroscopic properties of nuclear levels.

ACKNOWLEDGMENTS

The authors thank M. Korun, I. Lajovic, G. Strobl, M. Tiringer, and Z. Zorko for their help in taking and analyzing data. Thanks are also due to A. Brinšek, F. Detter, D. Hošnjak, and A. Ropret for technical assistance in preparing and running the experiment.

---

†Work supported by the Boris Kidrič Foundation.

[1]D. Brajnik, D. Jamnik, G. Kernel, U. Miklavžič, and J. Šnajder, Nucl. Instrum. 103, 189 (1972).

[2]J. S. Pruitt, A. Allisy, G. Joyet, W. Pohlit, M. Tubiana, and Č. Zupančič, J. Res. Natl. Bur. Stand. (U. S.) 66C, 107 (1962).

[3]Weighting was based on deexcitation γ-ray data.

[4]W. M. Mason, N. W. Tanner, and G. Kernel, Nucl. Phys. A138, 253 (1969).

[5]S. S. Hanna, H. F. Glavish, E. M. Diener, J. R. Calarco, C. C. Chang, R. Avida, and R. N. Boyd, Phys. Lett. 40B, 631 (1972).

[6]S. S. Hanna, in *Nuclear Structure Studies Using Electron Scattering and Photoreaction*, edited by K. Shoda and H. Ui (Tomizawa, Sendai, Japan, 1972), p. 453.

[7]A. S. Penfold and J. E. Leiss, Phys. Rev. 114, 132 (1959); and Analysis of photo cross sections (University of Illinois, May, 1958).

[8]W. Kessel, R. Bass, and R. Wechsung, Nucl. Phys. A206, 193 (1973), and references cited therein.

[9]J. S. Lopes, B. C. Robertson, R. D. Gill, R. A. I. Bell, and H. J. Rose, Nucl. Phys. A109, 241 (1968).

[10]D. B. Nichols and M. B. McEllistrem, Phys. Rev. 166, 1074 (1968).

[11]B. C. Robertson, Can. J. Phys. 49, 3051 (1971).

[12]This formula was deduced from a general expression of S. Devons and L. J. B. Goldfarb, in *Encyclopedia of Physics*, edited by S. Flügge (Springer, Berlin, 1957), Vol. 42, p. 362.

[13]H. J. Rose and D. M. Brink, Rev. Mod. Phys. 30, 306 (1967).

[14]S. A. E. Johansson and B. Forkman, Nucl. Phys. 36, 141 (1962).

[15]N. W. Tanner, G. C. Thomas, and E. D. Earle, Nucl. Phys. 52, 29 (1964).

[16]J. C. Hafele, F. W. Bingham, and J. S. Allen, Phys. Rev. 135, B365 (1964).

[17]L. Feldman, B. B. Baliga, and M. Nessin, Phys. Rev. 157, 921 (1967).

[18]K. Shoda, K. Abe, T. Ishizuka, N. Kawamura, M. Oyamada, and Baik-Nung Sung, J. Phys. Soc. Jap. 25, 664 (1968).

[19]J. Bartko and T. T. Thwaites, Phys. Lett. 27B, 212 (1969).

[20]C. P. Wu, J. E. E. Baglin, F. W. K. Firk, and T. W. Phillips, Phys. Lett. 29B, 359 (1969).

[21]F. Heimlich and W. Mausberg, Z. Phys. 231, 397 (1970).

[22]E. M. Diener, J. F. Amann, and P. Paul, Phys. Rev. C 7, 695 (1973).

[23]W. R. Dodge and W. C. Barber, Phys. Rev. 127, 1746 (1962).

[24]R. G. Allas, S. S. Hanna, L. Meyer-Schützmeister, and R. E. Segel, Nucl. Phys. 58, 122 (1964).

[25]G. Kernel and W. M. Mason, Nucl. Phys. A123, 205 (1969).

[26]N. Bezić, D. Jamnik, G. Kernel, J. Krajnik, and J. Šnajder, Nucl. Phys. A117, 124 (1968).

[27]M. Marangoni and A. M. Saruis, Nucl. Phys. A132, 649 (1969); and private communication.

[28]R. F. Barrett, L. C. Biedenharn, M. Danos, P. P. Delsanto, W. Greiner, and H. G. Wahsweiler, Rev. Mod. Phys. 45, 44 (1973).

[29]S. Hinds and R. Middleton, Nucl. Phys. 84, 651 (1966).

[30]G. R. Satchler, D. D. Armstrong, A. G. Blair, E. R. Flynn, R. J. Philpott, and W. T. Pinkston, Phys. Rev. 182, 1141 (1969).

[31]M. E. Cage, R. R. Johnson, P. D. Kunz, and D. A. Lind, Nucl. Phys. A162, 657 (1971).

[32]W. J. Gerace and A. M. Green, Nucl. Phys. A93, 110 (1967).

[33]W. J. Gerace and A. M. Green, Nucl. Phys. A123, 241 (1969).

[34]L. Zamick, Ann. Phys. (N.Y.) 47, 182 (1968).

[35]L. B. Hubbard, J. B. McGrory, and H. P. Jolly, Phys. Rev. C 6, 532 (1972).

[36]V. Gillet and E. A. Sanderson, Nucl. Phys. A91, 292 (1967).

[37]D. Agassi, V. Gillet, and A. Lumbruso, Nucl. Phys. A130, 129 (1969).

[38]T. A. Belote, A. Sperduto, and W. W. Buechner, Phys. Rev. 139, B80 (1965).

[39]T. A. Belote, W. E. Dorenbusch, and J. Rapaport, Nucl. Phys. A120, 401 (1968).

[40]H. T. Fortune, N. G. Puttaswamy, and J. L. Yntema,

Phys. Rev. 185, 1546 (1969).
[41]T. Erikson, Nucl. Phys. A205, 593 (1973).
[42]V. Gillet and E. A. Sanderson, Nucl. Phys. 54, 472 (1964).
[43]D. E. Frederick, Nucl. Phys. A101, 250 (1967).
[44]F. C. Barker and A. K. Mann, Phil. Mag. 2, 5 (1957).
[45]D. Brajnik, to be published.
[46]J. L. Durell, V. Metag, R. Repnow, A. N. James, J. F. Sharpey-Schafer, and P. von Brentano, Phys. Rev. Lett. 28, 1723 (1972).
[47]B. Elbek, A. Budzanowski, K. Grotowski, A. Kobos, A. Strzalkowski, and S. Wiktor, Nucl. Phys. A187, 355 (1972).
[48]D. Cline, W. Parker Alford, and L. M. Blau, Nucl. Phys. 73, 33 (1965).
[49]R. Bock, H. H. Duhm, and R. Stock, Phys. Lett. 18, 61 (1965).
[50]F. C. Erné, Nucl. Phys. 84, 91 (1966).
[51]S. Maripuu and G. A. Hokken, Nucl. Phys. A141, 481 (1970).
[52]R. M. Topphorn, M. Kregar, and G. G. Seaman, Phys. Rev. C 3, 2232 (1971).
[53]P. Goode and L. Zamick, Nucl. Phys. A129, 81 (1969).
[54]M. B. Lewis, Phys. Lett. 27B, 13 (1968).
[55]H. Ullrich and H. Krauth, Nucl. Phys. A123, 641 (1969).
[56]The approximate value 0.5 for the branching ratio follows from the assignment of the 2.60-MeV line in the deexcitation spectra (Fig. 3) to the cascade decay 5.62→3.02 MeV in ^{39}K rather than to 3.63 MeV→g.s. in ^{39}Ca (see Ref. 1). The assignment is supported by the following two reasons: First, there is no full-energy peak observed for the decay of the 3.63-MeV state. Second, the population of the analog state in ^{39}K at 3.59 MeV (Fig. 3) is found to be weak; consequently, the population of the 3.63-MeV state is expected to be even weaker due to the high threshold for the photoneutron reaction.
[57]J. C. Hiebert, E. Newman, and R. H. Basel, Phys. Rev. 154, 898 (1967).
[58]S. Fujii, Nucl. Phys. A132, 385 (1969).